OXFORD

Cerebral Cortex, 2016; 1–12

doi: 10.1093/cercor/bhw389
Original Article

ORIGINAL ARTICLE

Spatiotemporal Dynamics of Attention Networks Revealed by Representational Similarity Analysis of EEG and fMRI

V. Salmela[1,2], E. Salo[1,2], J. Salmi[1,2,3] and K. Alho[1,2]

[1]Division of Cognitive Psychology and Neuropsychology, Institute of Behavioral Sciences, University of Helsinki, FI-00014 Helsinki, Finland, [2]Advanced Magnetic Imaging Centre, Aalto NeuroImaging, Aalto University, Espoo FI-00076, Finland and [3]Faculty of Arts, Psychology and Theology, Åbo Akademi University, FI-20500 Turku, Finland

Address correspondence to Viljami Salmela. Email: viljami.salmela@helsinki.fi

Abstract

The fronto-parietal attention networks have been extensively studied with functional magnetic resonance imaging (fMRI), but spatiotemporal dynamics of these networks are not well understood. We measured event-related potentials (ERPs) with electroencephalography (EEG) and collected fMRI data from identical experiments where participants performed visual and auditory discrimination tasks separately or simultaneously and with or without distractors. To overcome the low temporal resolution of fMRI, we used a novel ERP-based application of multivariate representational similarity analysis (RSA) to parse time-averaged fMRI pattern activity into distinct spatial maps that each corresponded, in representational structure, to a short temporal ERP segment. Discriminant analysis of ERP-fMRI correlations revealed 8 cortical networks—2 sensory, 3 attention, and 3 other—segregated by 4 orthogonal, temporally multifaceted and spatially distributed functions. We interpret these functions as 4 spatiotemporal components of attention: modality-dependent and stimulus-driven orienting, top-down control, mode transition, and response preparation, selection and execution.

Key words: attention, brain networks, EEG, fMRI, representational similarity analysis

Introduction

Resolving the cerebral underpinnings of attention is one of the key questions in cognitive neuroscience (Petersen and Posner 2012). However, the distributed nature of higher level cognition poses challenges for research: attentional processes involve a number of cortical (Corbetta and Shulman 2002) and subcortical (Wimmer et al. 2015) structures, which could all have their own temporal processing scales (Gonzalez-Castillo et al. 2012). In addition, largely overlapping brain networks are activated by different attentional functions (Duncan 2010). Functional magnetic resonance imaging (fMRI) during attention demanding tasks has indicated that brain areas participating in these networks are located in the intra- and temporo-parietal, and superior and inferior frontal cortices (Corbetta and Shulman 2002). Even individual differences in attention can be predicted on the basis of connectivity in these networks (Rosenberg et al. 2016). Functional connections between these network areas persist in spontaneous activity measured during resting state without any designated task instructions given to the participants (Fox et al. 2006; Dosenbach et al. 2007; Yeo et al. 2011). Thus, fMRI data during task performance and rest demonstrate comparable spatial networks, but the relatively sluggish blood oxygenation level-dependent signal (Logothetis 2008) is not sufficient in unraveling the fine-grained temporal dynamics of attentional processes within these networks.

The models of attention supported by fMRI and behavioral studies have segregated attention-related bottom-up and top-down processes (Corbetta and Shulman 2002; Petersen and

Posner 2012). While attention modulates sensory processing of both visual and auditory target objects (Petkov et al. 2004; Johnson and Zatorre 2006; Pestilli et al. 2011), there may be intermodal differences in the networks guiding these modulations. In the visual modality, separate but interacting fronto-parietal networks have been found for top-down controlled and bottom-up triggered attention shifts (Corbetta and Shulman 2002; Petersen and Posner 2012). Subsequently, in the auditory modality top-down and bottom-up attention networks are presumably more overlapping (Salmi et al. 2009; Alho et al. 2015). Moreover, some areas of the top-down networks might be more related to divided than selective attention (Johnson and Zatorre 2006) or shifting attention between modalities (Shomstein and Yantis 2004; Salo et al. 2015). In addition, some networks activated during attention demanding tasks might be involved in task-related memory functions (Petersen and Posner 2012; Wallis et al. 2015) rather than attention. As compared with fMRI, more precise temporal information on attentional processes is provided by event-related potentials (ERPs) measured with electroencephalography (EEG). ERP studies have demonstrated attention-related modulations of sensory processing beginning already at 100 ms from stimulus onset (Hillyard et al. 1973; Näätänen et al. 1978; Woods et al. 1992; Mangun 1995) as well as distraction (Squires et al. 1975; Knight 1997; Escera et al. 1998; Fogelson et al. 2009), orienting (Hopf and Mangun 2000; Nobre et al. 2000; Salmi et al. 2007), or reorienting (Schröger and Wolff 1998; Berti and Schröger 2001) related responses between 200 and 600 ms from stimulus onset.

Despite extensive research knowledge on the specific brain areas and temporal components of attention, there is still a lack of studies describing spatiotemporal dynamics of attention networks and representational relations of the multiple attention-related processes. Answering these questions calls for specific methods that enable combining both spatially and temporally accurate neuroimaging techniques and experimental setups containing multiple conditions that are controlled for features not directly linked to attention, such as task difficulty. Integrating localization of cortical networks and their temporal dynamics is possible by combining fMRI and EEG measurements (Huster et al. 2012). EEG-based modeling of fMRI data has provided important knowledge, for example, by revealing brainstem connections to cortical attention networks around 200 and 450 ms after stimulus onset (Walz et al. 2013) as well as task- and response-related temporal dynamics in the frontal cortex and in the so-called default mode areas (Greicius et al. 2003; Walz et al. 2014). The advances of data analysis methods and multivariate pattern analysis (MVPA) have enabled separating distinct processes within overlapping brain networks, for example, segregating spatial and feature-based attention shifts (Greenberg et al. 2010) in the medial superior parietal lobule (Esterman et al. 2009). In the present study, we utilized representational similarity analysis (RSA) (Kriegeskorte et al. 2008; Kriegeskorte and Kievit 2013) to investigate spatiotemporal dynamics of attention networks. With RSA, we combined ERP and fMRI data from identical experiments by projecting both data sets into a common representational space, and investigated representational similarity of multiple attentional processes.

We collected ERP and fMRI data during a continuous 1-back adaptive pitch and orientation discrimination tasks performed separately or simultaneously by the participants at 70% threshold (Fig. 1). The experiments contained 18 different event types

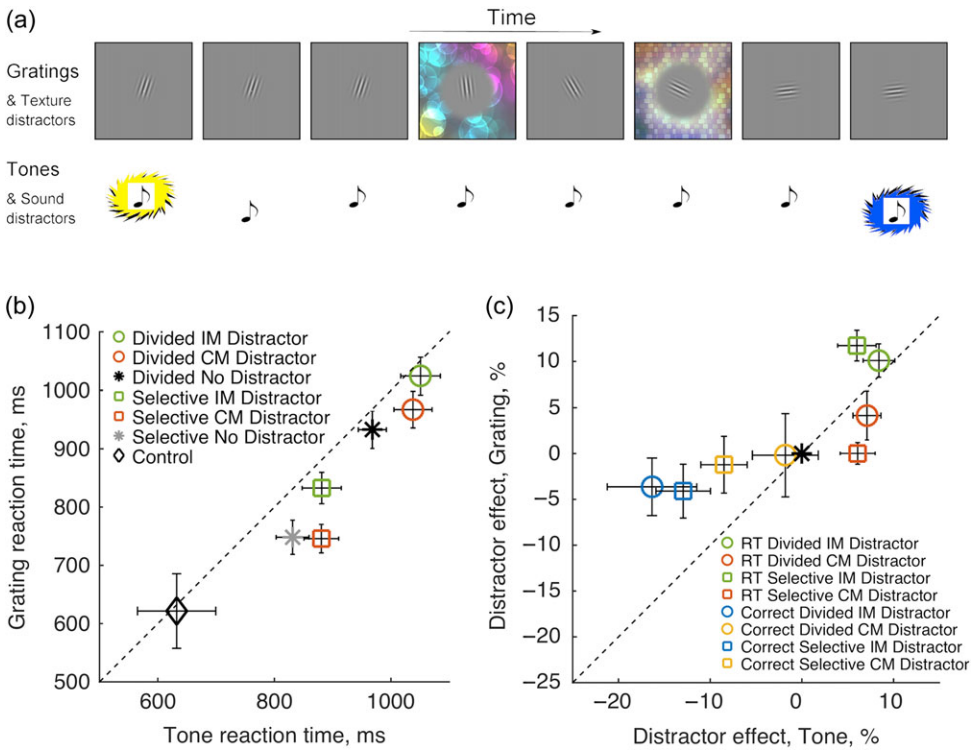

Figure 1. Experimental setup and behavioral results. (*a*) On each trial, both sinewave tone and sinewave grating were presented, and either tone pitch or grating orientation changed in relation to the previous trial. On 1/3 trials, either a visual distractor (spectrally complex texture) or an auditory distractor (spectrally complex sound) was presented. These distractors were intramodal (IM) or crossmodal (CM) with respect to the target event (pitch or orientation change). Error bars depict standard errors of mean. (*b*) RTs to tones and gratings. RTs were shortest in the control condition (black diamond), longer in the selective attention condition (squares, gray asterisk), and the longest in the divided attention condition (circles, black asterisk). (*c*) Distractor effect on discrimination of tones and gratings. Relative prolongation of RTs and decrease in proportion of correct responses in relation to targets without distractors (black asterisk). IM distractors (green and blue symbols) exhibited stronger effects than CM distractors (red and yellow symbols).

based on 2 × 3 × 3 factorial design (Table 1): Target Modality (auditory or visual), Attention Mode (selective or divided attention, or control task, i.e., a simple reaction time [RT] task), and Distractor Type (intramodal, crossmodal, or no distractor). With searchlight (Kriegeskorte et al. 2006) RSA we identified regional voxel clusters in fMRI data that contained representational structures similar to the representational structures calculated from short temporal segments of ERPs (Fig. 2). This resulted in a temporal ERP-fMRI correlation profile for each voxel and region (Fig. 3). Discriminant analysis of temporal profiles revealed 4 temporally multifaceted and spatially distributed functional components: 1) modality-dependent and stimulus-driven orienting of attention, 2) top-down guided attentional control, 3) shifting between attention and default modes, and 4) response selection, preparation, and execution (Fig. 4).

Materials and Methods

Participants

Thirteen healthy right-handed volunteers (7 females, mean ± standard deviation [SD] age 26 ± 6 years) with normal or corrected-to-normal vision and without known hearing deficits participated in both EEG and fMRI experiments. The participants gave a written informed consent before participating in the experiments approved by the Ethics Review Board in the Humanities and Social and Behavioural Sciences of the University of Helsinki.

Stimuli

The auditory stimuli were binaural sinewave tones and various spectrally complex sounds occurring simultaneously with a tone on some trials. The tones had an intensity of 80 dB sound pressure level (SPL), and duration of 300 ms including 10 ms linear onsets and offsets. The frequency of tones varied between 600 and 1800 Hz, either randomly or according to participants' correct/incorrect responses in the staircase procedure. The maximum change in pitch between consecutive trials was limited to 0.5 octaves. Complex synthetic sounds, such as clicks and ringtones, were used as auditory distractors. The maximum intensity of these distractor sounds was 80 dB SPL and they were low- and high-pass filtered with cutoffs at 7000 and 200 Hz, respectively. In addition, the distractor sounds were notch-filtered at 1000 Hz (filter width 2 octaves) to avoid acoustic masking of target tone frequencies. Each auditory distractor occurred only once during the experiment.

Visual stimuli were grayscale sinewave gratings and various colored textures occurring simultaneously with a grating on some trials. Each high-contrast grating was shown for 300 ms in a Gaussian envelope (diameter 3°). The spatial frequency of grating was 2 c/deg and the phase was randomly set in each trial. The orientation of grating was varied randomly (in conditions with no visual task) or according to participants' correct/incorrect responses in the staircase procedure. The lower part of the grating was kept at the center of the screen and the grating was rotated between 0 and 360°. However, the maximum change between consecutive trials was limited to 90°. The textures (size 16 × 24°) were used as visual distractors. To avoid spatial masking and to keep gratings identical across conditions, a circular 6° area was cut off from the center of distractor textures. The rms (root-mean-squared) contrast (SD of luminance divided with mean luminance) of the visual distractors was 0.3. Each visual distractor occurred only once during the experiment.

Procedure

The experiment consisted of auditory and visual 1-back discrimination tasks. The participants' auditory task was to indicate whether the pitch of the tone was higher or lower than the pitch of the preceding tone by pressing a button up or down with their right hand. The participants' visual task was to indicate whether the orientation of the grating rotated clock-wise or counter clock-wise in comparison with the preceding grating by pressing a button right or left with their right hand. A tone-grating pair was presented on each trial. The pairs were

Table 1 Experimental setup

Event	Block	Task	Target	Change in	Distractor	Trials in block
1	1	Selective attention: 1-back discrimination in one modality	Auditory	Tone	None	20
2					Auditory	5
3					Visual	5
4	2		Visual	Grating	None	20
5					Auditory	5
6					Visual	5
7	3	Divided attention: 1-back discrimination in both modalities	Auditory	Tone	None	20
8					Auditory	5
9					Visual	5
10			Visual	Grating	None	20
11					Auditory	5
12					Visual	5
13	4	Control: Press button for any stimuli	Both	Tone	None	20
14					Auditory	5
15					Visual	5
16				Grating	None	20
17					Auditory	5
18					Visual	5

Note: Eighteen trial types/events occurred in 4 different blocks. The experiment contained 3 task conditions: selective auditory, selective visual, and divided Attention Modes, as well as a control task. In the attention tasks, the target (to-be-discriminated change in tone pitch or grating orientation) was either auditory or visual. Some trials included an auditory or visual distractor.

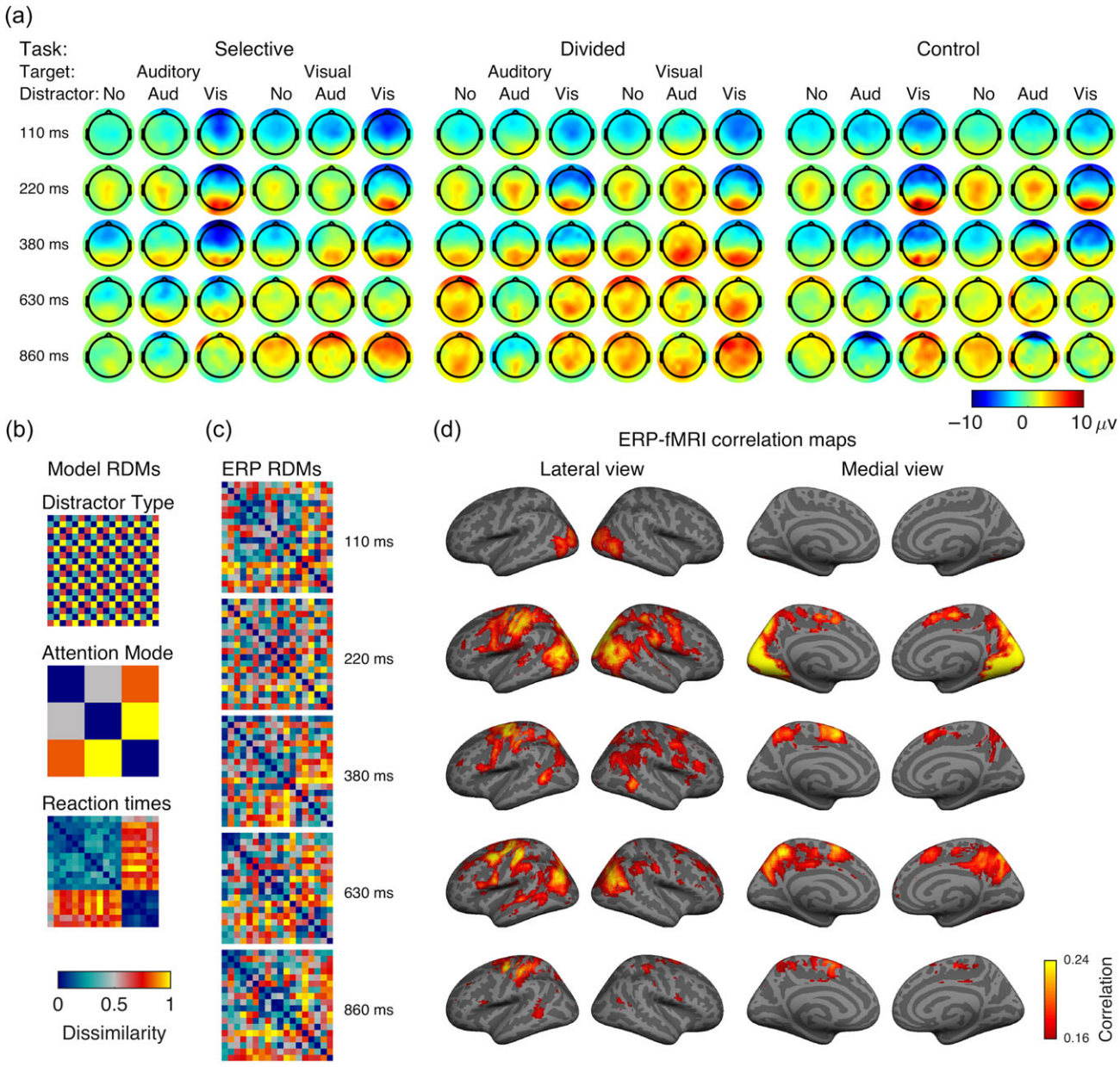

Figure 2. Results of the RSA of EEG and fMRI data at 5 time points from 110 to 860 ms after stimulus onset. (*a*) ERPs were calculated from the EEG by averaging epochs time-locked to stimulus events. Topographic maps of ERPs (the head viewed from above with the nose pointing upwards) averaged across participants. Aud = auditory, Vis = visual. (*b*) Model RDMs showing the expected effects of Distractor Type and Attention Mode, and an RDM calculated from RTs. (*c*) ERP RDMs were calculated by cross-correlating ERPs from all 64 channels across the 18 different experimental conditions within consecutive 10 ms segments from −200 to 1000 ms from stimulus onset, resulting in 120 RDMs. (*d*) ERP-fMRI correlation maps. fMRI data were analyzed with General Linear Model (GLM) containing separate regressors for each stimulus event and by calculating *t* values for each regressor in each voxel using statistical parametric mapping (SPM). First, fMRI RDMs were calculated by cross-correlating regressor *t* values of the 18 experimental events across voxels within a spherical searchlight, and then correlated with each ERP RDM (permutation test, $P < 0.05$). Supplementary Video 1 shows the full data from −200 to 1000 ms from stimulus onset.

presented sequentially with a constant onset-to-onset interval of 1.8 s. The magnitude of attended pitch and orientation change was determined using an adaptive staircase method with a 2-1 rule: after an incorrect response, the pitch/orientation difference between successive trials was increased and after 2 consecutive correct responses the pitch/orientation difference was decreased in steps of 3° and 0.01 octaves. This method produced a 70.7% discrimination threshold. Only trials without distractors were included in the staircase and the initial change was 15° and 0.1 octaves. Until the second reversal point, the amount of change was 3-fold. The average of the reversal points (the first 2 reversal points were excluded) was used as the discrimination threshold. The tones and gratings were created and their timing was controlled with Presentation software (Neurobehavioral Systems, www.neurobs.com).

In every condition, both tones and gratings were presented, but the participants' task was varied. The tone and grating discrimination tasks were performed separately ("selective attention" condition) or simultaneously ("divided attention" condition). In the divided attention condition, the stimulus was

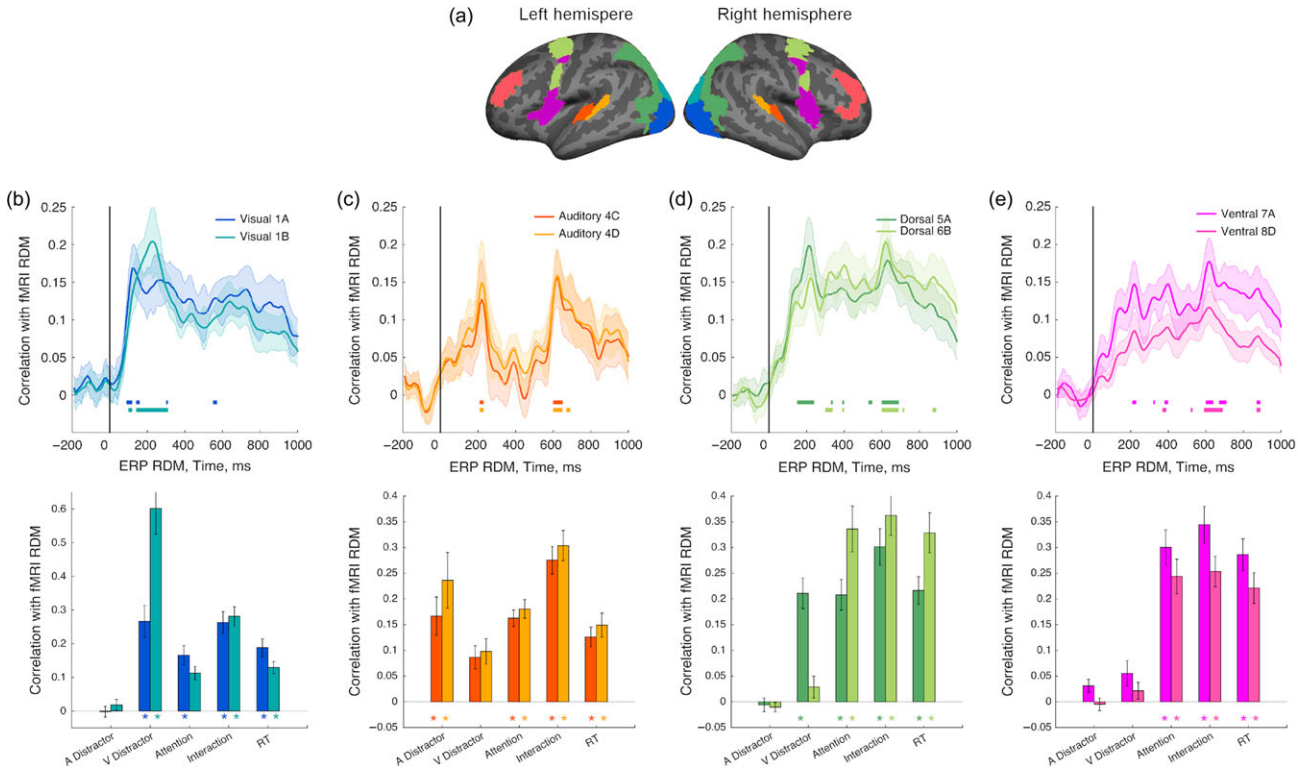

Figure 3. ROI analysis for 8 regions in 4 networks (*a*). In both hemispheres, each of the 17 resting state-defined networks (Yeo et al. 2011) were divided into 1–4 subregions according to lobes and anatomical structures (Destrieux et al. 2010). The resulting 44 ROIs were averaged across hemispheres. Temporal profiles (top row) from ERP-fMRI RSA and model correlations (bottom row) averaged across voxels. Straight lines and asterisks indicate statistically significant correlations (*t*-test, $P < 0.05$). Shaded area and error bars depict standard errors of mean. A = auditory, V = visual. Results are shown for (*b*) visual cortex, (*c*) auditory cortex, (*d*) dorsal attention network, and (*e*) ventral attention network.

changed in only one modality. Thus, in the divided attention condition, the participant had to first detect the modality in which the stimulus changed and then to decide to which direction the change had occurred. The selective attention conditions also contained sham trials in which the stimulus changed in the nonattended modality as well. These trials were discarded from the analysis in order to keep selective attention conditions similar to divided attention condition. In the control condition, the participants were asked to press a button whenever the tone-grating pair occurred. During all tasks, on 1/6 of the trials, a visual distractor and on another 1/6 of the trials an auditory distractor was presented with this pair.

In total, there were 18 different trial types in 4 experimental blocks (Table 1): 1) Auditory selective attention, 2) Visual selective attention, 3) Divided attention, and 4) Control. Each condition included in the present analysis (for excluded conditions, see below) contained 6 different combinations of target and distractor stimuli: 1) Auditory target without distractor, 2) Auditory target with auditory distractor, 3) Auditory target with visual distractor, 4) Visual target without distractor, 5) Visual target with auditory distractor, and 6) Visual target with visual distractor.

Each task consisted of 60 trials occurring in a random order: 40 trials without distractors, 10 trials with auditory distractor, and 10 trials with visual distractor. Different tasks were performed in different blocks, and the order of blocks was randomized in each run. Each run also contained single modality trials, which included visual and auditory tasks without stimuli in the other modality. These trials were excluded from all present analyses. Each participant took first part in the EEG and then in the fMRI experiment, and completed 3 runs in each experiment.

EEG Acquisition, Preprocessing, and ERP Analysis

The EEG data were acquired with Biosemi ActiveTwo system (BioSemi, Netherlands) with 64 scalp electrodes and 6 additional electrodes (at the right and left mastoids, at the canthi for horizontal electro-oculography, and above and below the left eye for vertical electro-oculography from the left eye). The EEG data were analyzed with EEGLAB toolbox (Delorme and Makeig 2004) and custom Matlab scripts. The EEG data were high-pass filtered using a cutoff of 0.5 Hz and low-pass filtered using a cutoff of 20 Hz. Bad channels were rejected manually and using an EEGLAB automatic channel rejection tool based on channel kurtosis. EEG data were sliced to 1200 ms epochs beginning 200 ms before each stimulus pair onset. Mean voltage during the 200-ms prestimulus period was used as the baseline. Independent components were calculated using FastIca algorithm (Hyvärinen 1999) and artifact components were removed using ADJUST toolbox (Mognon et al. 2011) after which the epochs were averaged to obtain ERPs to different events.

fMRI Acquisition, Preprocessing, and GLM Analysis

fMRI data were measured with a Siemens MAGNETOM Skyra 3T scanner (Siemens Healthcare) using 30-channel head coil. Three functional runs were measured using a gradient-echo echo planar imaging sequence (time repetition [TR] 1900 ms, time echo [TE] 32 ms, flip angle 75°, voxel matrix 64 × 64, field of view 20 cm, slice thickness 3.0 mm, in-plane resolution 3.1 mm × 3.1 mm × 3.0 mm). The functional measurements

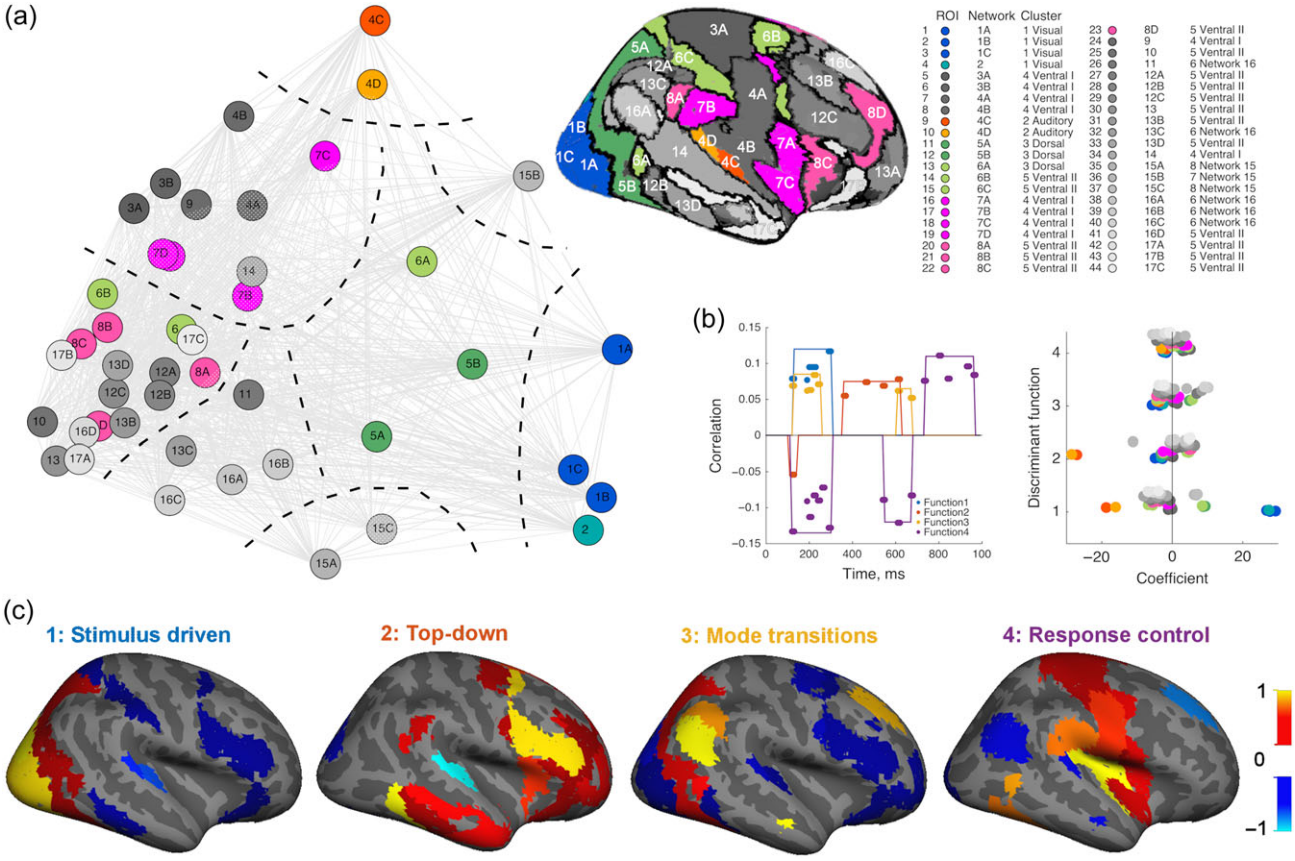

Figure 4. Spatiotemporal attention components. The data for the right and left hemispheres were averaged in the analysis. (*a*) Multidimensional scaling of temporal RDM of ROIs. Numbers and colors indicate resting state-based networks (Yeo et al. 2011) and letters A–D subregions of networks. Dashed black lines indicate cluster boundaries: Visual (Networks 1–2, blue), auditory (Network 4, orange), dorsal attention (Networks 5–6, green), ventral attention I (Network 7, pink), and ventral attention II (Network 8, red). (*b*) Correlation of discriminant functions and time points, and distribution of discriminant function coefficients. (*c*) Spatial maps of discriminant function coefficients (results based on data combined across the hemispheres projected on the lateral surface of the right hemisphere).

consisted of 388 volumes. To reach stable magnetization, the first 4 volumes were discarded from the analysis. A fast structural MR image with a 3D T1-weighted sequence (1 mm slice thickness) was acquired before the third functional run.

The fMRI data were analyzed with SPM12 Matlab toolbox (Penny et al. 2006), Freesurfer (Dale et al. 1999) software package, RSA toolbox (Nili et al. 2014), and custom Matlab scripts. In the preprocessing, the acquisition order of functional images and the head motion were corrected. Then, a standard GLM analysis was conducted using 35 regressors, one for each event type (18 regressors), and nuisance regressors for instructions (1), motion (6) and control conditions (10) that were excluded from the data analysis (one modality and sham trials). The resulting SPM_T images for 18 trial types were then analyzed using RSA.

Representational Similarity Analysis

For both ERP and fMRI data, we conducted an RSA (Kriegeskorte et al. 2008; Kriegeskorte and Kievit 2013). In the analysis, a representational dissimilarity matrix (RDM) was calculated by cross-correlating the measured data across 18 different trial types. For ERP data, the RDMs were calculated from all channels with consecutive 10 ms time windows. For fMRI data, a searchlight method (Kriegeskorte et al. 2006) was used and the RDMs were calculated from voxels within spherical searchlights (radius 3 voxels; volume ca. 100 voxels). The ERP and fMRI RDMs were then compared with each other, and with model RDMs based on the classification of experimental conditions according to Attention Mode and Distractor Type as well as on RTs and correct responses. For each model, we obtained a temporal activity profile based on the ERP data and a spatial correlation map based on the fMRI data. The statistical inference was calculated using *t*-tests and permutation tests. In permutations tests, data labels were shuffled and a distribution of correlations was calculated based on 5000 (ERP) or 1000 (fMRI) permutations to find correlation values that correspond to the top 5% of the simulated distributions.

Region of Interest and Discriminant Analyses

The correlations between ERPs and fMRI obtained in RSA were further analyzed with region of interest (ROI) analysis. A total of 44 ROIs were selected by first intersecting 17 networks found in resting-state analysis (Yeo et al. 2011) and 74 anatomical regions (Destrieux et al. 2010) that contained at least 100 common vertices, and then averaging some of the nearby regions in order to keep the number of ROIs reasonable. For each ROI, we averaged fMRI RDM correlations with ERP and model RDMs across voxels. RSA was applied to the temporal profiles of ROIs, and then multidimensional scaling was applied to the obtained RDM. The multidimensional scaling revealed 8 clusters, and this classification was then used in a step-wise discriminant analysis to find discriminant functions that maximized

Mahalanobis distances between the clusters. The resulting discriminant functions were evaluated by finding the highest/lowest correlations between the functions and the analyzed time points, as well as comparing the function coefficients across ROIs.

Results

Behavioral Performance

The effect of experimental manipulations on behavioral measures was tested with a repeated measures analysis of variance (ANOVA). The Imaging Modality (EEG vs. fMRI experiment) did not affect discrimination thresholds ($F_{1,12} = 1.31$, $P = 0.274$), RTs ($F_{1,12} = 1.160$, $P = 0.303$), or correct responses ($F_{1,12} = 0.739$, $P = 0.407$), and there were no significant interaction effects of the Imaging Modality and the other variables on thresholds or correct responses. However, for RTs, 2 significant interactions were found. In fMRI, but not in EEG, the RTs were longer to tones than gratings (Imaging Modality × Target Modality: $F_{1,12} = 17.19$, $P = 0.001$), especially in selective attention condition (Imaging Modality × Target Modality × Attention Mode: $F_{2,24} = 9.10$, $P = 0.007$). Since there were no main effects on Imaging Modality, the behavioral data from the EEG and fMRI experiments were combined for further analysis.

For both pitch and orientation discrimination (Fig. 1*a*), the thresholds increased to approximately 2-fold ($F_{1,12} = 14.96$, $P < 0.01$) during divided attention (pitch: 0.06 oct; orientation 9.5°) in relation to selective attention (pitch: 0.03 oct; orientation 5.4°). In the divided attention condition, the thresholds correlated positively between the modalities ($r = 0.53$, $P = 0.064$) showing that the participants did not pay more attention to one modality at the expense of another.

RTs increased as the task demands increased from the control task to the selective and divided Attention Modes (Fig. 1*b*; $F_{2,24} = 23.10$, $P < 0.001$). Adding a distractor to the tone-grating pair increased RTs significantly ($F_{2,24} = 31.09$, $P < 0.001$), especially when the distractor was within the same modality as the target stimulus (Fig. 1*b*, green symbols; Target Modality × Distractor Type interaction $F_{2,24} = 9.58$, $P < 0.01$). There was also a significant Attention Mode × Target Modality interaction ($F_{2,24} = 6.49$, $P < 0.01$) and Attention Mode × Target Modality × Distractor Type interaction ($F_{4,48} = 2.58$, $P < 0.05$), due to different effects of distractors on discriminating the tones and gratings in the selective and divided attention conditions. Specifically, crossmodal distractors did not prolong RTs to gratings in the selective attention condition (Fig. 1*b*), and the difference between effects of intramodal and crossmodal distractors was larger for the gratings than tones (Fig. 1*c*), while overall RTs were shorter for the gratings than tones ($F_{1,12} = 21.05$, $P < 0.01$).

There were no significant differences in the proportions of correct responses between the tones and gratings ($F_{1,12} = 1.17$, $P = 0.30$), but performance was less accurate during divided than selective attention ($F_{1,12} = 10.55$, $P < 0.01$). The distractors decreased the amount of correct responses (Fig. 1*c*; $F_{2,24} = 5.85$, $P < 0.01$), especially distractors in the target modality ($F_{2,24} = 6.22$, $P < 0.01$). The distractors tended to have a smaller effect on discrimination accuracy for gratings than tones (Fig. 1*c*), but this interaction was not statistically significant.

Event-related Potentials

The topographic ERP maps for all 18 events at 5 different time points are shown in Figure 2*a*. The ERPs within 110 ms after stimulus onset were highly similar (first row). At 220 ms (second row), comparison of trials without a distractor and with an auditory or visual distractor showed differing anterior–posterior distributions of activity (Fig. 2*a*). In comparison to distribution without distractors ("No" columns), the activity distribution was shifted to anterior regions during auditory distractors ("Aud" columns) and to posterior regions during visual distractors ("Vis" columns). Beginning at 380 ms (rows 3–5), differences related to the Attention Mode were found. Higher amplitudes were found in the selective (the 6 leftmost columns) and divided (6 columns in the middle) attention conditions than in the control condition (the 6 rightmost columns). Further, at 630 and 860 ms, the divided attention condition showed stronger responses than the selective attention conditions.

ERP-fMRI Correlations

The RSA is based on RDMs calculated by cross-correlating variables of interest. A specific RDM shows rank order of dissimilarities that can be compared with RDMs based on models or RDMs derived from data collected with another method. Example model RDMs corresponding to the effects of Distractor Type and Attention Mode are shown in Figure 2*b*, as well as an RDM calculated from the present RT data. Dissimilarities of ERP amplitude distributions (Fig. 2*a*) were quantified with RDMs (Fig. 2*c*). From these RDMs, dissimilarities related to Distractor Type can be seen as a grid in the matrix (e.g., visual distractors: rows and columns 3, 6, 9. in the matrix) and dissimilarities related to Attention Mode as blocks, that is, differences between rows/columns 1–6 (selective attention) versus rows/columns 7–12 (divided attention) versus rows/columns 13–18 (control condition).

A searchlight RSA was conducted by calculating correlations between each ERP RDM and fMRI RDM within the spherical searchlights (radius 3 voxels). The fMRI RDMs were calculated from SPM_T images, regressor *t* values based on statistical parametric mapping that did not contain any temporal information as such. The analysis revealed distinct spatial correlation maps for different time points showing spreading of activity from sensory to parietal regions and further to frontal regions and propagation of activity back to the parietal and sensory regions (Fig. 2*d*). The highest correlations for ERP RDMs calculated at 110 ms were found in a voxel cluster located in the visual cortex (first row). At 220 ms (second row), the most prominent correlations spread to the parietal regions, auditory cortex, and to the medial visual cortex. At 380 ms (third row), the correlations in the visual cortex were diminished and both parietal and frontal regions showed correlation maxima. At 630 and 860 ms (rows 4 and 5), high correlations were found in frontal voxel clusters, mainly in motor and supplementary motor areas at 860 ms, as well as in some clusters in the visual temporo-occipito-parietal areas.

In order to further confirm that the ERP-fMRI activity pattern correlations were related to attentional processes, we conducted a model based RSA (Supplementary Fig. 1*a*) separately for the ERP and fMRI data. Distractor Type model correlations showed transient correlation peaks at 185, 220, and 290 ms after stimulus onset in ERPs (Supplementary Fig. 1*b*) and indicated significant voxel clusters in the visual and auditory cortices in fMRI (Supplementary Fig. 1*c*). In contrast, classification of trials on the basis of Attention Mode or RTs revealed sustained correlations at longer latencies in ERPs, starting around 400 ms (Supplementary Fig. 1*b*) and in fMRI correlations were localized to parietal and frontal regions, and to the temporo-parietal junction (Supplementary Fig. 1*c*). Model based on correct responses did not reveal any significant ERP correlations or voxel clusters in fMRI.

We used all 64 measured EEG channels in our analysis. To ensure that this did not influence the results and to test whether selecting a subset of electrodes could be used in investigating specific responses, we conducted similar analysis with 6 subsets of electrodes: 1) 34 anterior electrodes, 2) 29 posterior electrodes, 3) 13 frontal electrodes, 4) 10 parietal electrodes, 5) 11 occipital electrodes, and 6) sparse set of 16 electrodes across the scalp (Supplementary Fig. 2*b*). With the electrode subsets, reduced correlations with model RDMs were found, with only a few statistically significant differences to the original data (Supplementary Fig. 2*c*). Importantly, reducing the number of EEG channels removed some of the effects found with the full electrode set, but did not produce any new effects or correlation peaks. With the standard 16 channel setup, the results were virtually identical (Supplementary Fig. 2*c*) to the original analysis. Similarly to the ERP and model RDM correlations, no additional voxel clusters were found in ERP-fMRI correlations, and the subsets revealed only some of the voxels found with the full 64 channels set (Supplementary Video 2). Taken together, these results suggest that the number of EEG electrodes used in the ERP-fMRI RSA is not critical as long as the electrodes are sparsely distributed and little is gained by reducing the number of electrodes.

Temporal Similarity

To fully characterize the spatiotemporal dynamics of attention-related cortical areas, we conducted region of interest (ROI) analyses based on networks defined by resting-state analysis (Yeo et al. 2011) and cortical anatomy (Destrieux et al. 2010). For each of the 44 ROIs, we calculated average correlation with ERP RDMs, to reveal the time course of activity in the given ROI, as well as average correlation with model RDMs, to reveal the ROIs function in relation to Distractor Type (auditory, visual, or no distractor), Attention Modes, Distractor Type × Attention Mode interaction, and Behavior (RTs). No systematic differences between the hemispheres were found and therefore results for the left and right hemispheres were averaged. Our main interest was to find temporal dissimilarities in auditory and visual network as well as attention networks. Thus, we focused on 8 ROIs (Fig. 3*a*), 2 in each of these networks: Networks 1 (visual), 4 (auditory), 5–6 (dorsal attention), and 7–8 (ventral attention).

In the visual areas of Network 1 (Fig. 3*a*, blue) the ERP-fMRI correlations rose steeply, starting at 100–120 ms, and reached peak values between 110 and 310 ms (Fig. 3*b*). After the transient peak, the correlations gradually decreased. In these areas, the highest correlation was found for the Visual Distractor model, suggesting that the dissimilarities within these areas were mainly related to distractor processing, but significant correlations were also found for Attention Mode and Distractor Type × Attention Mode interaction. A quite different pattern of results was found in the auditory areas of Network 4 (Fig. 3*a*, orange): in Heschl's gyrus and the planum temporale, 2 sharp correlation peaks were found at 220–230 ms and 600–650 ms, and after both peaks the correlations decreased sharply (Fig. 3*c*). The model correlations suggested that these areas were involved in processing of Auditory Distractors and also showed Distractor Type × Attention Mode interaction.

In the parietal areas of dorsal attention Networks 5 and 6 (Fig. 3*a*, green), the correlations started to increase at 140–160 ms and 2 peaks were found at 160–240 and 530–680 ms (Fig. 3*d*). These areas were related to processing of Visual Distractors and to Attention Mode, and especially to interaction of Distractor Type and Attention Mode. In the frontal areas of the ventral attention Networks, that is, Networks 7 and 8 (Fig. 3*a*, pink/red), the correlations increased gradually and 3/4 correlation peaks were found at 220–230, 380–400, 580–690, and 870–880 ms (Fig. 3*e*). Within these areas, no correlation with distractor models was found, but instead the areas correlated with Attention Mode, Distractor Type × Attention Mode interaction and RT models, suggesting a role of these frontal regions in attentional control.

Spatiotemporal Attention Components

To test temporal similarities between all ROIs, we conducted RSA for their temporal profiles (some shown in Fig. 3*b*–*e*) and applied multidimensional scaling of the resulting RDM (Fig. 4*a*). Temporal similarity across analyzed ROIs suggested 8 cortical clusters (Fig. 4*a*, dashed lines): 1) visual Networks 1–2, 2) auditory regions of Network 4, 3) dorsal attention Network 5 (and area in Network 6), 4) ventral attention Network 7 (and areas in Networks 3, 4, 9, 14), 5) ventral attention Network 8 (and areas in Networks 6, 10, 12, 13, 16, 17), 6) Networks 11, 13, 16, and 7–8) 2 clusters from Network 15. The temporal profile of each ROI was then subjected to discriminant analysis based on the 8 clusters.

The discriminant analysis revealed 7 statistically significant, orthogonal functions. The first 4 functions explained 95% of the variance across areas (57%, 26%, 9%, and 3% for the Functions 1–4, respectively). Discriminant Function 1 correlated positively with time points between 130 and 300 ms (Fig. 4*b*, blue line), and Function 2 correlated negatively with an early time point of 130 ms and positively with late time points between 370 and 620 ms (Fig. 4*b*, red line). Function 3 also had 2 phases, and correlated positively with early (130–270 ms) and late (620–680 ms) time points (Fig. 4*b*, yellow line). Function 4 had 3 phases: a negative correlation with earlier (130–300 ms) and later (550–680 ms) time points, as well as a positive correlation with very late (740–970 ms) time points (Fig. 4*b*, purple line). Spatially, Function 1 separated sensory cortical regions from fronto-parietal areas, as well as the auditory and visual regions from each other, and Function 2 segregated the sensory from frontal regions (Fig. 4*b*). The variance explained by Functions 3 and 4 was smaller and consequently, these functions did not segregate areas as clearly as the first 2 functions when plotted on the same scale (Fig. 4*b*). Overall, the 4 determined discriminant functions essentially capture dissimilarity between the temporal profiles of ROIs (Fig. 3) and explain the observed spatial similarity structure (Fig. 4*a*).

To further visualize the differences in spatial and temporal activation characteristics, the discriminant function coefficients on each ROI were plotted on the cortical surface (Fig. 4*c*). The early time scale and sensory-frontal division of Function 1 suggests that it is related to stimulus-driven processing, which depended on the modality. The later time course of Function 2 and the high coefficient for it in frontal areas indicates that this function relates to top-down guided attentional control. The time course of Function 3 appears to represent shifting from the default mode (Greicius et al. 2003) to the Attention Mode and back to the default mode, since the highest coefficients were found in the default mode areas. The 3 phases of Function 4 and the high coefficients in the sensory-motor areas might indicate that it is associated with response preparation, selection and execution after target occurrence, and perhaps with preparation for the next trial. Since each experimental condition had a motor response, purely motor processes should not show up in the analysis.

Discussion

We combined ERP and fMRI data with a novel application of RSA in order to resolve spatiotemporal dynamics of cortical networks related to multiple attentional processes. The ERP RDMs revealed topographic dissimilarities across all experimental conditions and these were compared with RDMs within the fMRI searchlight voxel clusters. We were able to parse the fMRI data into several spatial maps corresponding to short temporal segments of ERPs. The present results reveal complex temporal dynamics of attentional processes with a few separable processing phases. Distractor-related pattern correlations were found in the sensory areas at early time window of 200 ms from audiovisual stimulus onset. Early peaks were also found from parietal and frontal areas, and our model analysis indicated that these were related to interaction of the Attention Mode and Distractor Type, but not to distractor processing as such. In addition to the early peak, dorsal parietal areas showed elevated correlations also at a later time point of 600 ms, related to distractor processing as well as to the interaction of Attention Mode and Distractor Type. Elevated pattern correlations in the ventral parietal regions and frontal areas were found at 4 distinct time points, around 200, 400, 600, and 800 ms, showing the role of these areas in attentional control during all phases of the cognitive tasks. The results suggest that the spatial activity patterns in fMRI data contain information from several time points, and that this information can be recovered using external temporal ERP markers. Furthermore, multidimensional scaling of temporal profiles suggested 8 spatial networks: 2 sensory, 3 attention, and 3 other networks. Discriminant analysis of these 8 networks revealed 4 orthogonal components that each had separate temporal profiles and spatial distributions. Our results suggest 4 distinct spatiotemporal components for attention: modality-dependent and stimulus-driven orienting, top-down guided control of attention, brain state transitions, and response selection, planning and execution.

Temporal resolution of fMRI has fundamental limitations and it probably will not reach a millisecond scale of ERPs even in the future although it has improved considerably in the past decades (Logothetis 2008). We resolved the lack of high temporal resolution by combing the temporal ERP and spatial fMRI data with RSA. Previously, RSA has been used to combine fMRI and magnetoencephalography (MEG) for studying spatiotemporal processing of tones (Su et al. 2014) and visual objects (Cichy et al. 2014). We guided our searchlight (Kriegeskorte et al. 2006) fMRI analysis with ERP-based RDMs and investigated spatiotemporal dynamics of attention across the entire cortex. Thus, our analysis revealed spatial maps of representational relationships that correlated with certain time points in electrophysiological brain activity, and hence inform us about the time course of attentional processing. The success in our endeavor might be partly due to the fact that ERPs are quite specific with regard to stimulus processing and attention functions examined in the present study. This would have not been the case with nonaveraged EEG signal. Similarly, instead of raw time series we used regressors derived from the fMRI data. Thus, the event-related averaging ensured high quality signals for the RSA.

In our experimental setup, we calculated discrimination thresholds, RTs, and correct responses. All these behavioral measures confirmed that the present attention and distractor manipulations were as effective as expected and that the participants' task performance was similar in the ERP and fMRI experiments. The EEG experiment was always conducted before the fMRI experiment. Nevertheless, there were no differences in task performance that could reflect, for instance, learning. Perhaps, the less comfortable and acoustically noisy environment of fMRI canceled any learning-related improvements in performance. Our behavioral tasks consisted of low-level (perceptual) components of pitch and orientation discrimination as well as higher level (cognitive) components of response selection, focusing and dividing attention. The low-level component of the task was adaptively varied in order to control for the task difficulty. In the model RSA, no significant voxel clusters were found for model RDM calculated from correct responses, suggesting that the adaptive method was effective. However, for model RDM calculated from RTs, significant clusters were found in locations comparable with the Attention Mode model. This suggests that the RTs reflect, in addition to perceptual discriminability, cognitive processes related to decision making, attention and response preparation. The decision making cascade involves several brain areas and components with different temporal dynamics (Philiastides et al. 2014; Muraskin et al. 2016). The top-down attention and response control components found in our discrimination analysis likely involve processes related also to decision making.

Separate model correlations confirmed that the temporal and spatial patterns in ERPs and fMRI, respectively, were indeed related to Distractor Types, Attention Modes, and their interaction. Overall, we found stronger correlations between fMRI and model RDMs than between fMRI and ERP RDMs. However, spatial distribution for some of the models was more limited; Attention Mode and Distractor models mainly segregated frontal areas from auditory and visual areas. We also tried other models, such as separating auditory and visual targets in addition to separating Attention Modes, but the correlations were not significantly affected. In contrast, the spatial distributions of ERP correlations varied markedly and revealed several distinct spatial clusters at different time points. Correlation map most comparable to ERP-fMRI correlations was found for model depicting interaction of Attention Mode and Distractors, thus confirming that our ERP-fMRI correlations were genuinely related to attention and distractor processing.

We parsed time-averaged fMRI data into several distinct spatial maps depicting spatiotemporal dynamics of attentional processing. The resolution of our regional temporal correlation profiles calculated from fMRI data was comparable to ERPs, even though we used time-averaged SPM_T images. Since these images integrate activation over a few seconds, the information from different time points within the spatial patterns could have been significantly blurred or smoothed. However, our results suggest that the fMRI activation patterns at different time points add up, and hence the spatial information at different times is recoverable. Therefore, we propose that spatiotemporal dynamics of whole brain fMRI activity patterns can be investigated with spatiotemporal models that include separate components for each time point of interest.

Overall, stronger ERP-fMRI correlations were found in the visual than in auditory cortex, and the early part of correlations showed visual cortex activity first, followed by parietal and auditory cortex activity. These could be due to visual dominance during multisensory stimuli, for example, ventriloquism effect (Driver 1996). Another possibility is that our visual stimuli just elicited stronger effects than auditory stimuli, or that the auditory stimuli and responses were partly masked more by the scanner noise and responses to it, respectively. A third possibility is that spatial activation patterns are more persistent in the visual than in auditory cortex, for example,

due to differences in functional organization between the visual and auditory cortices. Furthermore, the observed temporal profiles for visual and auditory areas were also different. In the visual areas, only one early peak was found and the correlation decreased gradually, whereas in the auditory areas, 2 separate transient peaks were found, suggesting that attention modulates visual and auditory regions differently. Behaviorally, crossmodal distractors had a smaller effect on grating than tone discrimination. This suggests that the difference around 600 ms between the visual and auditory cortices might be related to modality switching or reorienting. Furthermore, there was an asymmetry of behavioral responses between the modalities: the distractors prolonged the RTs to gratings relatively more than the RTs to tones, and reduced the amount of correct responses relatively more for the tones than gratings. This asymmetry might reflect the previously reported distractor-related differences between the modalities (Boll and Berti 2009; Bendixen et al. 2010), and especially the biases toward top-down and bottom-up attention systems in the visual and auditory modalities, respectively (Braga et al. 2016). After the sensory-parietal responses, complex dynamics emerged involving response-related processing, fronto-parietal, and default mode networks. Interestingly, the peaks in ERP-fMRI correlations occurred roughly at the same time points in separate areas of cortical networks. Thus instead of the classical serial and hierarchical processing account, our results are consistent with previous research suggesting dynamic attentional control involving distinct components, which have several phases and are distributed to multiple cortical areas.

The present multidimensional scaling and discriminant analysis suggested 4 spatiotemporal components. In addition to the components related to cognitive processing, we also found components related to shifting between brain states and response control. The first component, modality-dependent and stimulus-driven orienting, corresponding to the early peaks around 200–300 ms of ERP-fMRI correlations, is likely related to the components of the P3a ERP response associated with novelty detection and involuntary attention (Yago et al. 2003) and to ERP modulations due to attentional selection of the target events for further processing (Bengson et al. 2015). The second component, top-down guided control, corresponding to the later peaks of ERP-fMRI correlations at 400–600 ms is likely to be associated with ERP responses related to reorienting of attention (Schröger and Wolff 1998; Berti and Schröger 2001) and other late attentional processes (Hopf and Mangun 2000; Nobre et al. 2000; Bengson et al. 2015). The first and second components are roughly consistent with the dorsal and ventral attention networks (Corbetta and Shulman 2002), but they were not limited only to the areas of these networks. Although the determined spatiotemporal components were orthogonal, they still occasionally recruited overlapping cortical areas, in agreement with previous reports showing parallel, partly overlapping attention networks (Stoppel et al. 2013). The time scales of these correlations are consistent with attention-related connections found in a study with a simultaneous EEG-fMRI recording (Walz et al. 2013). The third and fourth components, apparently corresponding to brain state transitions and response control, respectively, are consistent with previous EEG-based modeling of fMRI task and response-related effects in the frontal cortex and default mode areas (Walz et al. 2014) as well as the opposing effects of attention and default mode networks (Anderson et al. 2011; Hellyer et al. 2014).

Instead of sustained brain activity on the time scale of seconds or tens of seconds during different tasks, we used an event-related design to study attentional functions occurring within 1 s from stimulus onset. Furthermore, we used MVPA to find dissimilarities in local activity distributions, not in the mean activity, during multiple attentional processes. In our MVPA, we found similar networks in both hemispheres, and observed larger attentional modulations to distractors than targets. Inclusion of both auditory and visual attention conditions may have emphasized supramodal attention networks. Moreover, previous studies suggest that attention effects spread between synchronously stimulated modalities (Degerman et al. 2007) perhaps explaining the present similarity of target responses across different attention instructions. We also found robust pattern correlations in the prefrontal areas. MVPAs are more sensitive than univariate analyses (Kriegeskorte and Kievit 2013), which might explain the lack of prefrontal activation during some attention tasks in previous studies. In our experiment, we used an adaptive task to individually control for task difficulty. Specific attentional functions may have different effects on brain responses: task difficulty or required effort is observed as an increase in total activity, whereas the task type, such as focused or divided attention, would be specifically reflected in the activation patterns. Thus, due to the adaptive task our results likely emphasize task type-related activity changes.

Our results show that the spatial patterns of time-averaged fMRI data contain information at a subsecond time scale and that this information can be recovered using temporal information from ERPs. This suggests that the fMRI activity patterns could be modeled with spatiotemporal models that include different pattern predictions for different time points, that is, the activity patterns within each searchlight or ROI could be modeled as a sum of multiple predicted patterns. Developing a quantitative spatiotemporal model would be a significant future step in understanding the complex dynamics of supramodal attention. In the present study, the spatiotemporal dynamics of attention suggested 4 multifaceted and spatially distributed components related to stimulus-driven and top-down controlled attention, shifting between brain states and response control.

Supplementary Material

Supplementary material can be found at *Cerebral Cortex* online.

Funding

Academy of Finland (grants #260054 and #297848).

Notes

Conflict of Interest: None declared.

References

Alho K, Salmi J, Koistinen S, Salonen O, Rinne T. 2015. Top-down controlled and bottom-up triggered orienting of auditory attention to pitch activate overlapping brain networks. Brain Res. 1626:136–145.

Anderson JS, Ferguson MA, Lopez-Larson M, Yurgelun-Todd D. 2011. Connectivity gradients between the default mode and attention control networks. Brain Connect. 1:147–157.

Bendixen A, Grimm S, Deouell LY, Wetzel N, Madebach A, Schroger E. 2010. The time-course of auditory and visual

distraction effects in a new crossmodal paradigm. Neuropsychologia. 48:2130–2139.
Bengson JJ, Kelley TA, Mangun GR. 2015. The neural correlates of volitional attention: a combined fMRI and ERP study. Hum Brain Mapp. 36:2443–2454.
Berti S, Schröger E. 2001. A comparison of auditory and visual distraction effects: behavioral and event-related indices. Brain Res Cogn Brain Res. 10:265–273.
Boll S, Berti S. 2009. Distraction of task-relevant information processing by irrelevant changes in auditory, visual, and bimodal stimulus features: a behavioral and event-related potential study. Psychophysiology. 46:645–654.
Braga RM, Hellyer PJ, Wise RJ, Leech R. 2016. Auditory and visual connectivity gradients in frontoparietal cortex. Hum Brain Mapp. doi:10.1002/hbm.23358.
Cichy RM, Pantazis D, Oliva A. 2014. Resolving human object recognition in space and time. Nat Neurosci. 17:455–462.
Corbetta M, Shulman GL. 2002. Control of goal-directed and stimulus-driven attention in the brain. Nat Rev Neurosci. 3: 201–215.
Dale AM, Fischl B, Sereno MI. 1999. Cortical surface-based analysis. I. Segmentation and surface reconstruction. Neuroimage. 9:179–194.
Degerman A, Rinne T, Pekkola J, Autti T, Jaaskelainen IP, Sams M, Alho K. 2007. Human brain activity associated with audiovisual perception and attention. Neuroimage. 34: 1683–1691.
Delorme A, Makeig S. 2004. EEGLAB: an open source toolbox for analysis of single-trial EEG dynamics including independent component analysis. J Neurosci Methods. 134:9–21.
Destrieux C, Fischl B, Dale A, Halgren E. 2010. Automatic parcellation of human cortical gyri and sulci using standard anatomical nomenclature. Neuroimage. 53:1–15.
Dosenbach NU, Fair DA, Miezin FM, Cohen AL, Wenger KK, Dosenbach RA, Fox MD, Snyder AZ, Vincent JL, Raichle ME, et al. 2007. Distinct brain networks for adaptive and stable task control in humans. Proc Natl Acad Sci U S A. 104: 11073–11078.
Driver J. 1996. Enhancement of selective listening by illusory mislocation of speech sounds due to lip-reading. Nature. 381:66–68.
Duncan J. 2010. The multiple-demand (MD) system of the primate brain: mental programs for intelligent behaviour. Trends Cogn Sci. 14:172–179.
Escera C, Alho K, Winkler I, Näätänen R. 1998. Neural mechanisms of involuntary attention to acoustic novelty and change. J Cogn Neurosci. 10:590–604.
Esterman M, Chiu YC, Tamber-Rosenau BJ, Yantis S. 2009. Decoding cognitive control in human parietal cortex. Proc Natl Acad Sci U S A. 106:17974–17979.
Fogelson N, Wang X, Lewis JB, Kishiyama MM, Ding M, Knight RT. 2009. Multimodal effects of local context on target detection: evidence from P3b. J Cogn Neurosci. 21:1680–1692.
Fox MD, Corbetta M, Snyder AZ, Vincent JL, Raichle ME. 2006. Spontaneous neuronal activity distinguishes human dorsal and ventral attention systems. Proc Natl Acad Sci U S A. 103: 10046–10051.
Gonzalez-Castillo J, Saad ZS, Handwerker DA, Inati SJ, Brenowitz N, Bandettini PA. 2012. Whole-brain, time-locked activation with simple tasks revealed using massive averaging and model-free analysis. Proc Natl Acad Sci U S A. 109:5487–5492.
Greenberg AS, Esterman M, Wilson D, Serences JT, Yantis S. 2010. Control of spatial and feature-based attention in frontoparietal cortex. J Neurosci. 30:14330–14339.
Greicius MD, Krasnow B, Reiss AL, Menon V. 2003. Functional connectivity in the resting brain: a network analysis of the default mode hypothesis. Proc Natl Acad Sci U S A. 100: 253–258.
Hellyer PJ, Shanahan M, Scott G, Wise RJ, Sharp DJ, Leech R. 2014. The control of global brain dynamics: opposing actions of frontoparietal control and default mode networks on attention. J Neurosci. 34:451–461.
Hillyard SA, Hink RF, Schwent VL, Picton TW. 1973. Electrical signs of selective attention in the human brain. Science. 182:177–180.
Hopf JM, Mangun GR. 2000. Shifting visual attention in space: an electrophysiological analysis using high spatial resolution mapping. Clin Neurophysiol. 111:1241–1257.
Huster RJ, Debener S, Eichele T, Herrmann CS. 2012. Methods for simultaneous EEG-fMRI: an introductory review. J Neurosci. 32:6053–6060.
Hyvärinen A. 1999. Fast and robust fixed-point algorithms for independent component analysis. IEEE Trans Neural Netw. 10:626–634.
Johnson JA, Zatorre RJ. 2006. Neural substrates for dividing and focusing attention between simultaneous auditory and visual events. Neuroimage. 31:1673–1681.
Knight RT. 1997. Distributed cortical network for visual attention. J Cogn Neurosci. 9:75–91.
Kriegeskorte N, Kievit RA. 2013. Representational geometry: integrating cognition, computation, and the brain. Trends Cogn Sci. 17:401–412.
Kriegeskorte N, Goebel R, Bandettini P. 2006. Information-based functional brain mapping. Proc Natl Acad Sci U S A. 103: 3863–3868.
Kriegeskorte N, Mur M, Bandettini P. 2008. Representational similarity analysis - connecting the branches of systems neuroscience. Front Syst Neurosci. 2:4.
Logothetis NK. 2008. What we can do and what we cannot do with fMRI. Nature. 453:869–878.
Mangun GR. 1995. Neural mechanisms of visual selective attention. Psychophysiology. 32:4–18.
Mognon A, Jovicich J, Bruzzone L, Buiatti M. 2011. ADJUST: an automatic EEG artifact detector based on the joint use of spatial and temporal features. Psychophysiology. 48:229–240.
Muraskin J, Brown T, Walz J, Conroy B, Goldman RI, Sajda P 2016. Imaging decision-related neural cascades in the human brain. bioRxiv.
Nili H, Wingfield C, Walther A, Su L, Marslen-Wilson W, Kriegeskorte N. 2014. A toolbox for representational similarity analysis. PLoS Comput Biol. 10:e1003553.
Nobre AC, Sebestyen GN, Miniussi C. 2000. The dynamics of shifting visuospatial attention revealed by event-related potentials. Neuropsychologia. 38:964–974.
Näätänen R, Gaillard AW, Mäntysalo S. 1978. Early selective-attention effect on evoked potential reinterpreted. Acta Psychol (Amst). 42:313–329.
Penny WD, Friston KJ, Ashburner JT, Kiebel SJ, Nichols TE. 2006. Statistical parametric mapping: the analysis of functional brain images. London: Elsevier Science.
Pestilli F, Carrasco M, Heeger DJ, Gardner JL. 2011. Attentional enhancement via selection and pooling of early sensory responses in human visual cortex. Neuron. 72:832–846.
Petersen SE, Posner MI. 2012. The attention system of the human brain: 20 years after. Annu Rev Neurosci. 35:73–89.
Petkov CI, Kang X, Alho K, Bertrand O, Yund EW, Woods DL. 2004. Attentional modulation of human auditory cortex. Nat Neurosci. 7:658–663.

Philiastides MG, Heekeren HR, Sajda P. 2014. Human scalp potentials reflect a mixture of decision-related signals during perceptual choices. J Neurosci. 34:16877–16889.

Rosenberg MD, Finn ES, Scheinost D, Papademetris X, Shen X, Constable RT, Chun MM. 2016. A neuromarker of sustained attention from whole-brain functional connectivity. Nat Neurosci. 19:165–171.

Salmi J, Rinne T, Degerman A, Alho K. 2007. Orienting and maintenance of spatial attention in audition and vision: an event-related brain potential study. Eur J Neurosci. 25: 3725–3733.

Salmi J, Rinne T, Koistinen S, Salonen O, Alho K. 2009. Brain networks of bottom-up triggered and top-down controlled shifting of auditory attention. Brain Res. 1286:155–164.

Salo E, Rinne T, Salonen O, Alho K. 2015. Brain activations during bimodal dual tasks depend on the nature and combination of component tasks. Front Hum Neurosci. 9:102.

Schröger E, Wolff C. 1998. Attentional orienting and reorienting is indicated by human event-related brain potentials. Neuroreport. 9:3355–3358.

Shomstein S, Yantis S. 2004. Control of attention shifts between vision and audition in human cortex. J Neurosci. 24: 10702–10706.

Squires NK, Squires KC, Hillyard SA. 1975. Two varieties of long-latency positive waves evoked by unpredictable auditory stimuli in man. Electroencephalogr Clin Neurophysiol. 38:387–401.

Stoppel CM, Boehler CN, Strumpf H, Krebs RM, Heinze HJ, Hopf JM, Schoenfeld MA. 2013. Distinct representations of attentional control during voluntary and stimulus-driven shifts across objects and locations. Cereb Cortex. 23:1351–1361.

Su L, Zulfiqar I, Jamshed F, Fonteneau E, Marslen-Wilson W. 2014. Mapping tonotopic organization in human temporal cortex: representational similarity analysis in EMEG source space. Front Neurosci. 8:368.

Wallis G, Stokes M, Cousijn H, Woolrich M, Nobre AC. 2015. Frontoparietal and cingulo-opercular networks play dissociable roles in control of working memory. J Cogn Neurosci. 27:2019–2034.

Walz JM, Goldman RI, Carapezza M, Muraskin J, Brown TR, Sajda P. 2013. Simultaneous EEG-fMRI reveals temporal evolution of coupling between supramodal cortical attention networks and the brainstem. J Neurosci. 33:19212–19222.

Walz JM, Goldman RI, Carapezza M, Muraskin J, Brown TR, Sajda P. 2014. Simultaneous EEG-fMRI reveals a temporal cascade of task-related and default-mode activations during a simple target detection task. Neuroimage. 102 (Pt 1):229–239.

Wimmer RD, Schmitt LI, Davidson TJ, Nakajima M, Deisseroth K, Halassa MM. 2015. Thalamic control of sensory selection in divided attention. Nature. 526:705–709.

Woods DL, Alho K, Algazi A. 1992. Intermodal selective attention. I. Effects on event-related potentials to lateralized auditory and visual stimuli. Electroencephalogr Clin Neurophysiol. 82:341–355.

Yago E, Escera C, Alho K, Giard MH, Serra-Grabulosa JM. 2003. Spatiotemporal dynamics of the auditory novelty-P3 event-related brain potential. Brain Res Cogn Brain Res. 16:383–390.

Yeo BT, Krienen FM, Sepulcre J, Sabuncu MR, Lashkari D, Hollinshead M, Roffman JL, Smoller JW, Zollei L, Polimeni JR, et al. 2011. The organization of the human cerebral cortex estimated by intrinsic functional connectivity. J Neurophysiol. 106:1125–1165.